



***PTEN*, a Putative Protein Tyrosine Phosphatase Gene Mutated in Human Brain, Breast, and Prostate Cancer**

Jing Li, *et al.*

*Science* **275**, 1943 (1997);

DOI: 10.1126/science.275.5308.1943

---

*This copy is for your personal, non-commercial use only.*

---

**If you wish to distribute this article to others**, you can order high-quality copies for your colleagues, clients, or customers by [clicking here](#).

**Permission to republish or repurpose articles or portions of articles** can be obtained by following the guidelines [here](#).

**The following resources related to this article are available online at [www.sciencemag.org](http://www.sciencemag.org) (this information is current as of December 19, 2011 ):**

**Updated information and services**, including high-resolution figures, can be found in the online version of this article at:

<http://www.sciencemag.org/content/275/5308/1943.full.html>

This article **cites 18 articles**, 9 of which can be accessed free:

<http://www.sciencemag.org/content/275/5308/1943.full.html#ref-list-1>

This article has been **cited by** 100 articles hosted by HighWire Press; see:

<http://www.sciencemag.org/content/275/5308/1943.full.html#related-urls>

Downloaded from [www.sciencemag.org](http://www.sciencemag.org) on December 19, 2011

- regions forming the basis for our ROIs with further support from cerebrocerebellar circuitry. For instance, the lateral neocerebellum sends output to the prefrontal cortex [F. A. Middleton and P. L. Strick, *Science* **266**, 458 (1994)]; the right prefrontal cortex is involved in attention tasks of the type we used [D. T. Stuss, T. Shallice, M. P. Alexander, T. W. Picton, *Ann. N.Y. Acad. Sci.* **769**, 191 (1995)]; and cerebellar input to the right cerebrum is from the left cerebellum [M. B. Carpenter, *Core Text of Neuroanatomy* (Williams & Wilkins, Baltimore, ed. 4, 1991)].
22. ROI drawing was guided by a human cerebellar atlas [G. A. Press, J. W. Murakami, E. Courchesne, M. Grafe, J. R. Hesselink, *Am. J. Neuroradiol.* **11**, 41 (1990)]. The Motor ROI was drawn from the surface location of the right primary fissure (pf) to the center of the band of white matter separating the anterior vermis (AVe) from the posterior vermis. From there, a line was drawn to the apex of the AVe. This ROI was completed by a line drawn along the surface of the cerebellum, back to the right pf. The Attention ROI was drawn from the surface location of the left pf to the center of the same white-matter band. A second line was drawn from this point to the surface location of the left horizontal fissure (hf). A line drawn along the surface of the cerebellum back to the left pf completed this ROI.
23. Because all stimuli were presented at a single spatial location in the center of foveal vision, eye movement activation was not predicted to occur. Moreover, previous work would predict that if eye movements had occurred, the resulting activation would occur in the cerebellar vermis [L. Petit *et al.*, *J. Neurosci.* **16**, 3714 (1996)], a region not activated during the Attention task. All areas that were active during the Attention task were also active during the Attention-with-Motor task, indicating that those behavioral requirements unique to the Attention task—namely, silent counting and encoding the number of targets—did not add to the results. Silent counting activation has been reported in the inferior cerebellum [E. Ryding, J. Decety, H. Sjöholm, G. Stenberg, D. H. Ingvar, *Brain Res. Cogn. Brain Res.* **1**, 94 (1993)] and in a “midline cerebellar region” [J. A. Fiez *et al.*, *J. Neurosci.* **16**, 808 (1996)]. In our study, the focus of attention activity was in the left cerebellar hemisphere, yet the right cerebellar hemisphere is consistently active during verbal tasks (12). Thus, nonverbal visual attention activated a side and region inconsistent with predicted silent counting effects. Still, to investigate whether silent counting might have contributed to these results, we instructed four subjects to silently count from 1 to 10 repeatedly in the absence of any visual stimuli. Examination of activation during this task revealed no cerebellar activation within the Attention VOI. Working memory activation of the cerebellum has also been reported (11), and the requirement to encode the number of targets during the Attention task placed minor demands on working memory. However, encoding the number targets was not required by the Attention-with-Motor task, and there were no regions of cerebellar activation unique to the Attention task as compared with the Attention-with-Motor task. Thus, like silent counting, working memory did not contribute to the activation effects observed during the Attention task.
24. In rats, when cerebellar stimulation occurs in advance of a sensory stimulus, neural responsiveness to that stimulus is altered at the brainstem, thalamic, hippocampal, and cortical levels (4, 5), and neural signal-to-noise enhancement can result (4); such effects are independent of the engagement of motor systems. For instance, when background luminance reduces to noise levels the colliculus response to a flash, stimulation of vermis lobules VI–VII causes the colliculus response to that flash to emerge above noise if stimulation occurs in advance of the visual stimulus (4).
25. M. G. Paulin, *Brain Behav. Evol.* **41**, 39 (1993).
26. J. C. Eccles, M. Ito, J. Szentagothai, *The Cerebellum as a Neuronal Machine* (Springer-Verlag, Berlin, 1967).
27. D. Flament, J. M. Ellermann, S.-G. Kim, K. Uğurbil, T. J. Ebner, *Hum. Brain Mapp.* **4**, 210 (1996); M. E. Raichle *et al.*, *Cereb. Cortex* **4**, 8 (1994).
28. S. L. Rao *et al.*, *Hum. Brain Mapp.* (suppl. 1), 412 (1995).
29. When sensory information is anticipated, attention is quickly and accurately redirected toward the predicted source of information. On the basis of neurobehavioral and neurophysiological evidence in patients with cerebellar lesions, it has been hypothesized that the cerebellum, through its connections with attention systems (2), influences the speed and accuracy of such attention changes (2, 9).
30. The cerebellum accomplishes this anticipatory function by encoding (“learning”) sequences of multidimensional information about external and internal events. A large body of evidence shows that the cerebellum may be involved in such learning [J. L. Raymond, S. G. Lisberger, M. D. Mauk, *Science* **272**, 1126 (1996)]. Whenever an analogous sequence begins to unfold, the cerebellum predicts what is about to happen, reads out the rest of the sequence, and triggers changes in the neural responsiveness of systems expected to be needed in upcoming moments (2, 9).
31. Anticipation involves predicting the internal conditions needed for a particular motor or mental operation and setting those conditions in preparation for that operation. Complete knowledge of upcoming events is not necessary; simple exposure to aspects of a stimulus that may soon arrive will trigger anticipatory responding of the cerebellum. The anticipatory response is neither a sensory nor a motor activity, but rather a general response that prepares whichever neural systems may be necessary in upcoming moments. An example may be changes in the vestibulo-ocular reflex (VOR) in anticipation of changes in vergence observed in the monkey [L. H. Snyder, D. M. Lawrence, W. M. King, *Vision Res.* **32**, 569 (1992)]. A model of how the cerebellum might mediate such anticipatory modulation of the VOR has been proposed [O. Coenen and T. J. Sejnowski, in *Advances in Neural Information Processing* 8, D. Touretzky, M. Mozer, M. Hasselmo, Eds. (MIT Press, Cambridge, MA, 1996), pp. 89–95].
32. To create functional maps, we interpolated the correlation coefficient images to match the resolution of anatomical images and registered them to the anatomical images to reduce warping. Next, through rotation, translation, and scaling, each subject’s cerebellum was transformed to a standard anatomical space by normalizing to a single subject chosen as the standard. All activated voxels were then superimposed across subjects for each task and slice.
33. We thank S. A. Hillyard, T. J. Sejnowski, and J. Townsend for helpful comments; L. Frank, D. Blaettler, and M. Belmonte for technical assistance; and the Santarsiero family for a generous donation. Supported by National Institute of Mental Health grant RO1-MH36840 (E.C.), a San Diego Children’s Hospital Research Center seed grant (G.A.), and a McDonnell-Pew Graduate Fellowship in Cognitive Neuroscience (G.A.).

4 December 1996; accepted 28 January 1997

## PTEN, a Putative Protein Tyrosine Phosphatase Gene Mutated in Human Brain, Breast, and Prostate Cancer

Jing Li,\* Clifford Yen,\* Danny Liaw,\* Katrina Podsypanina,\* Shikha Bose, Steven I. Wang, Janusz Puc, Christa Miliaris, Linda Rodgers, Richard McCombie, Sandra H. Bigner, Beppino C. Giovanella, Michael Ittmann, Ben Tycko, Hanina Hibshoosh, Michael H. Wigler, Ramon Parsons†

Mapping of homozygous deletions on human chromosome 10q23 has led to the isolation of a candidate tumor suppressor gene, *PTEN*, that appears to be mutated at considerable frequency in human cancers. In preliminary screens, mutations of *PTEN* were detected in 31% (13/42) of glioblastoma cell lines and xenografts, 100% (4/4) of prostate cancer cell lines, 6% (4/65) of breast cancer cell lines and xenografts, and 17% (3/18) of primary glioblastomas. The predicted *PTEN* product has a protein tyrosine phosphatase domain and extensive homology to tensin, a protein that interacts with actin filaments at focal adhesions. These homologies suggest that *PTEN* may suppress tumor cell growth by antagonizing protein tyrosine kinases and may regulate tumor cell invasion and metastasis through interactions at focal adhesions.

As tumors progress to more advanced stages, they acquire an increasing number of genetic alterations. One alteration that occurs at high frequency in a variety of human tumors is loss of heterozygosity (LOH) at chromosome 10q23. This change appears to occur late in tumor development: although rarely seen in low-grade glial tumors and early-stage prostate cancers, LOH at 10q23 occurs in ~70% of glioblastomas (the most advanced form of glial tumor) and ~60% of advanced prostate cancers (1, 2). This pattern of LOH, and the recent finding that wild-type chromosome 10 suppresses the tu-

morigenicity of glioblastoma cells in mice, suggest that 10q23 encodes a tumor suppressor gene (3).

To identify this putative tumor suppressor gene, we performed representational difference analysis (RDA) on 12 primary breast tumors (4). A probe, CY17, derived from one of the tumors was mapped to chromosome 10q23, near markers WI-9217 and WI-4264, on the Whitehead-MIT radiation hybrid map (5). To map the location of CY17 more precisely, we isolated three yeast artificial chromosomes (YACs) containing CY17 that are present on the

sequence tagged site (STS)-based map of the human genome (6, 7). These YACs placed CY17 slightly centromeric to the position determined by radiation hybridization and precisely identified its location (Fig. 1A). Analysis of 32 primary invasive breast cancers revealed LOH in this region in about 50% of the samples. No homozygous deletions of CY17 were detected in a panel of 65 breast tumor cell lines (25) and xenografts (40) (8), so eight additional markers were analyzed in the 10q23 region (D10S579, D10S215, AFMA086WG9, D10S541, AFM280WE1, WI-10275, WI-8733, WI-6971). We identified homozygous deletions of AFMA086WG9 in two xenografts, Bx11 and Bx38 (Figs. 1B and 2A) and then screened a bacterial artificial chromosome (BAC) library with this marker (9). Using new STSs from four independent BAC clones, we determined that the minimal region of deletion was within BAC C (Fig. 1B) (10). Homozygous deletions of AFMA086WG9 were also detected in two of eight glioblastoma cell lines, three of 34 glioblastoma xenografts, and two of four prostate cancer cell lines (11). One of the glioblastoma samples, cell line A172, had the same deletion pattern as the original breast xenografts; the deletions in the other samples were larger (Fig. 1B).

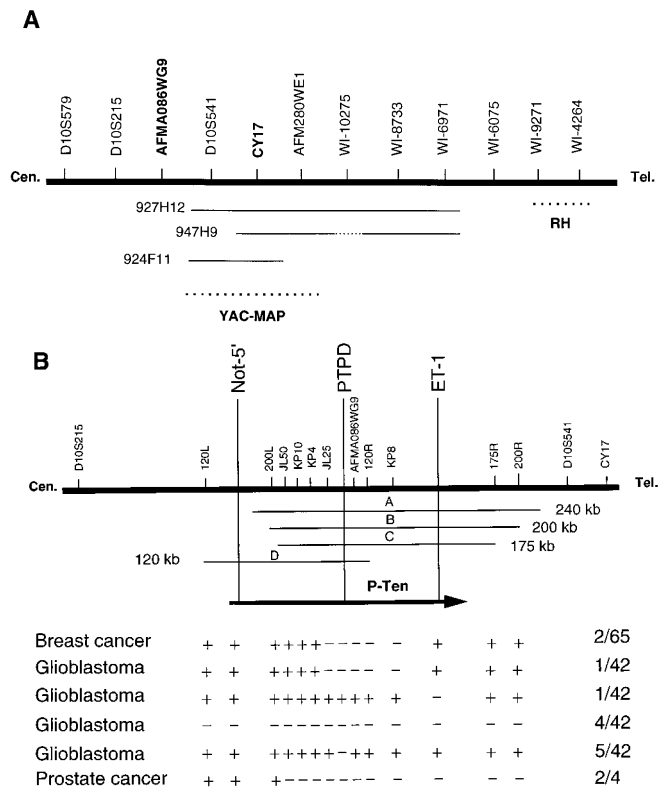
To confirm the presence of homozygous deletions, we hybridized a Southern (DNA) blot with a 3-kb probe derived from a genomic clone spanning the region of deletion (12). Xenografts anticipated to have a homozygous deletion did not hybridize to this probe; the control xenografts hybridized to the expected 3-kb band (Fig. 2B).

We identified genes within the 10q23 region by exon trap analysis of BACs C and D (Fig. 1B) (13). Two trapped exons, ET-1 and ET-2, had sequences that were perfect matches to an unmapped UNIGENE assembly of expressed sequence tags (ESTs) as well as several unassembled ESTs (6). Clones containing the ESTs were sequenced and used to assemble an open read-

ing frame (ORF) of 403 amino acids (Fig. 3A). To verify the location of this cDNA, we obtained the intronic sequence around ET-1 by directly sequencing BAC C. An STS primer pair (ET-1) was generated that mapped back to BACs A, B, and C (Fig. 1B). In addition, we screened the Map Panel #2 monochromosome human-rodent hybrid panel to confirm the unique location of this exon on chromosome 10 (14).

Our entire panel of tumor xenografts and cell lines was screened with this primer pair, and we identified an additional glioblastoma cell line (DBTRG-05MG) with a deletion of 180 base pairs (bp) (Fig. 1B) (Fig. 2C). Sequence analysis revealed that the deletion had removed 180 bp of exonic sequence and the splice donor site from this 225-bp exon. This deletion was not present in 52 normal blood samples or in more than

**Fig. 1.** Region of homozygous deletion on chromosome 10q23. **(A)** The STS-based YAC map of the region surrounding CY17. Marker locations are taken from the Whitehead STS-based map. RH indicates the radiation hybrid interval for CY17. CY17 positive YAC addresses are indicated. YAC map indicates the interval containing CY17 inferred from the YAC addresses. Cen., centromere; Tel., telomere. **(B)** Map of homozygous deletions on 10q23, showing the STS markers spanning the deleted region, the four BACs overlapping the region, and the location of *PTEN* with respect to the STS markers. STS markers Not-5', PTPD, and ET-1 contain exonic sequences of the *PTEN* gene. Absence of homozygous deletion is indicated with a "+" and presence of homozygous deletion with a "-." Numbers to the right indicate the fraction of tumor cell lines and xenografts with the deletion. The two breast cancer samples with a deletion are xenografts Bx11 and Bx38. Glioblastoma line A172 has a deletion encompassing markers JL25 through KP8 and glioblastoma line DBTRG-05MG has a deletion affecting only ET-1. The glioblastoma samples with a deletion across the entire region are the cell line U105 and xenografts 2, 3, and 11, and the samples with deletion of only PTPD, which contains the phosphatase domain, are xenografts 22, 23, 24, 25, and 32. The prostate cancer cell lines with homozygous deletions are NCI H660 and PC-3. The 5' end of the *PTEN* cDNA was determined to be coincidental with the Not I site 20 kb from the centromeric end of BAC D by sequence analysis. These maps are not drawn to scale.



J. Li, D. Liaw, K. Podsypanina, S. I. Wang, J. Puc, C. Millaresis, R. Parsons, Department of Pathology and Department of Medicine, College of Physicians & Surgeons, Columbia University, 630 West 168 Street, New York, NY 10032, USA.  
 C. Yen, L. Rodgers, R. McCombie, M. Wigler, Cold Spring Harbor Laboratory, Cold Spring Harbor, NY 11724, USA.  
 S. H. Bigner, Department of Pathology, Duke University Medical Center, Durham, NC 27710, USA.  
 B. Giovannella, Stehlin Foundation for Cancer Research, St. Joseph Hospital, Houston, TX 77003, USA.  
 M. Iltmann, New York VA Medical Center and Department of Pathology, New York University, 423 East 23 Street, New York, NY 10010, USA.  
 S. Bose, B. Tycko, H. Hibshoosh, Department of Pathology, College of Physicians & Surgeons, Columbia University, New York, NY 10032, USA.

\*These authors contributed equally to this work.  
 †To whom correspondence should be addressed.

**Table 1.** Summary of *PTEN* mutations in tumor cell lines and primary tumors.

Tumor sample	Tissue of origin	Codon	Mutation*	Predicted effect
LNCaP	Prostate	6	AAA to A	Frameshift
534T†	Glioblastoma	15	AGA to AGAGA	Frameshift
U87MG	Glioblastoma	54	49 bp deletion	Frameshift
MDA-MB-468	Breast	70	44 bp deletion	Frameshift
132T†	Glioblastoma	129	GGA to AGA	Gly to Arg
DU145	Prostate	134	ATG to TTG	Met to Leu
U373MG	Glioblastoma	241	TTT to TTT TT	Frameshift
BT549	Breast	274	GTA AAT to TAA AT	Stop
DBTRG-05MG‡	Glioblastoma	274-342	Delete 204 bp	In-frame deletion
134T†	Glioblastoma	337	4 bp deletion	Frameshift

\*Mutations are indicated in the sense orientation. †Primary tumors. All other samples are tumor cell lines. The mutations in the primary tumors were not found in matched blood DNA. ‡DBTRG-05MG has a genomic deletion of 180 bp within exon ET-1, which includes the splice donor site. Because of this deletion, the transcript contains an in-frame deletion of codons 274 to 342.

125 other primary tumors, xenografts, and cell lines tested.

Sequence analysis of the ORF revealed a protein tyrosine phosphatase domain (Fig. 3B) and a large region of homology (~175 amino acids) to chicken tensin and bovine auxilin (Fig. 3C). We therefore call the gene *PTEN* for Phosphatase and Tensin homolog deleted on chromosome Ten. The phosphatase domain of the P-TEN protein contained the critical (I/V)-H-C-X-A-G-X-X-R-(S/T)-G motif found in tyrosine and dual-specificity phosphatases (15). The phosphatase domain exon mapped within all four BACs and was deleted in all of the samples with homozygous deletions except for DBTRG-05MG. These results thus placed this exon within the region of homozygous deletion near JL25 and AFMA086WG9 (Fig. 1B). We then screened the remaining xenografts and cell lines for additional homozygous deletions and identified five more glioblastoma xenografts lacking this exon. These data indicate that the phosphatase domain encoded by *PTEN* was targeted for mutations in tumor xenografts and cell lines.

The phosphatase domain of P-TEN is most related in sequence to those of CDC14, PRL-1 (phosphatase of regenerating liver), and BVP (baculovirus phosphatase) (Fig. 3B). CDC14 and BVP are dual-specificity phosphatases that remove phosphate groups from tyrosine as well as serine and threonine (16). These phosphatases can be distinguished from the better characterized VH1-like enzymes by sequence differences outside of the core conserved domain. Both PRL-1 and CDC14 are involved in cell growth, and CDC14 appears to play a role in the initiation of DNA replication (17). In contrast to P-TEN, these phosphatases do not have extensive homology to tensin and auxilin. P-TEN is also homologous to the protein tyrosine phosphatase domains of three ORFs (Y50.2, PTP-IV1, CPTPH) whose protein products have not been characterized. Of these hypothetical proteins, only the putative yeast phosphatase Y50.2 has significant homology to tensin. Although tensin and auxilin are not expected to have phosphatase activity, they both contain elements of the protein tyrosine phosphatase signature sequence (18), which suggests that they may share a tertiary structure with these enzymes (19).

If *PTEN* is a tumor suppressor gene, the *PTEN* allele retained in tumor cells with LOH should contain inactivating mutations. To search for such mutations, we performed a protein truncation test on 20 breast, six glioblastoma, and two prostate tumor cell lines (20). Two truncating mutations in *PTEN* were identified in the breast samples (Table 1). BT549 cells had a 1-bp deletion of

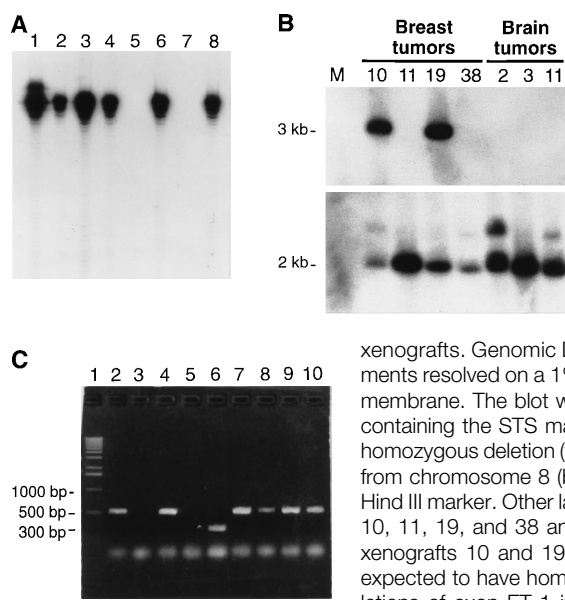


**Fig. 2.** Homozygous deletions in tumor cell lines and xenografts. **(A)** A 6% polyacrylamide sequencing gel showing the products of PCR amplification of AFMA086WG9 from breast cancer cell lines (lanes 1 to 4) and xenografts (lanes 5 to 8). Lane 1, MDA-MB-330; lane 2, MDA-MB-157; lane 3, MDA-MB-134-VI; and lane 4, MDA-MB-435S; lane 5, Bx11; lane 6, Bx15; lane 7, Bx38; and lane 8, Bx39. **(B)** Southern blot analysis of tumor xenografts. Genomic DNA was digested with Eco RI, the fragments resolved on a 1% agarose gel, and transferred to a nylon membrane. The blot was probed with a 3-kb Eco RI fragment containing the STS marker JL25, which is within the region of homozygous deletion (top), or to a second 2-kb Eco RI fragment from chromosome 8 (bottom). Lane M, bacteriophage lambda Hind III marker. Other lanes contain DNA from breast xenografts 10, 11, 19, and 38 and brain xenografts 2, 3, and 11. Breast xenografts 10 and 19 were loaded as controls and were not expected to have homozygous deletions. **(C)** Homozygous deletions of exon ET-1 in glioblastoma cell lines. Genomic DNA samples were PCR amplified using intronic primers that amplify exon ET-1. The products were resolved on a 1.2% agarose gel and then stained with ethidium bromide. Lane 1 contains a DNA marker. The remaining lanes contain PCR products from control templates and seven glioblastoma cell lines: lane 2, lymphocyte DNA; lane 3, water; lane 4, U118MG; lane 5, A172; lane 6, DBTRG-05MG; lane 7, U373; lane 8, T-98G; lane 9, U-87MG; and lane 10, U138MG. Full-length products are present for all templates except water, A172, and DBTRG-05MG.

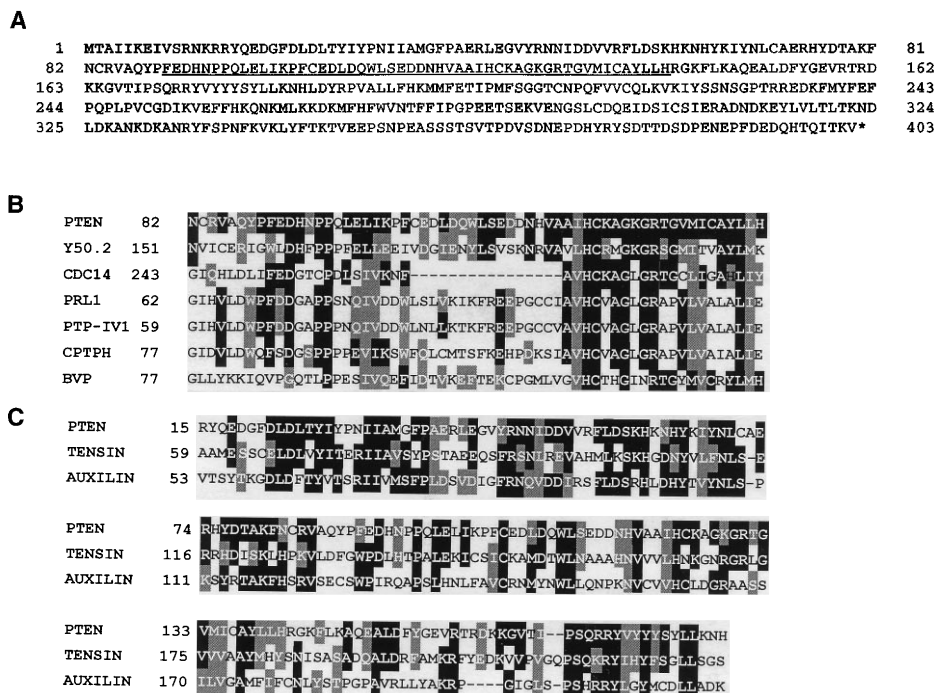


**Fig. 3.** **(A)** Predicted amino acid sequence of P-TEN. The putative phosphatase domain is underlined. The nucleotide sequence has been deposited in GenBank (accession number U93051). Abbreviations for amino acids are A, Ala; C, Cys; D, Asp; E, Glu; F, Phe; G, Gly; H, His; I, Ile; K, Lys; L, Leu; M, Met; N, Asn; P, Pro; Q, Gln; R, Arg; S, Ser; T, Thr; V, Val; W, Trp; and Y, Tyr. **(B)** Homology of P-TEN to protein tyrosine phosphatases. The sequence alignment was performed by ClustalW (<http://dot.imgen.bcm.tmc.edu:9331/multi-align/Options/clustalw.html>). The National Center for Biotechnology Information (NCBI) ID numbers are P53916 (Y50.2), M61194 (CDC14), A56059 (PRL1), 1246236 (PTP-IV1), 1125812 (CPTPH), and P24656 (BVP). Black boxes indicate amino acid identities and gray boxes indicate similarities. **(C)** Homology of P-TEN to chicken tensin and bovine auxilin. Alignment was performed as in (B) over the region of highest homology. NCBI ID numbers are A54970 (tensin) and 485269 (auxilin).

Downloaded from www.sciencemag.org on December 19, 2011

a G, leading to the formation of a stop codon TAA (Fig. 4A), and MDA-MB-468 cells had a deletion of 44 bp at codon 70, which resulted in a frameshift on the amino terminal side of the tyrosine phosphatase domain. Mutations in *PTEN* were also identified in three of the six glioblastoma cell lines: DBTRG-05MG cells had an in-frame deletion of 204 bp caused by the genomically deleted exon ET-1 (Fig. 4B), U373MG had a 2-bp insertion at codon 242, and U87MG had a frameshift at codon 54. Both of the prostate tumor cell lines had *PTEN* mutations: LNCaP cells had a 2-bp deletion at codon 6, leading to a frameshift (Fig. 4C), and DU145 cells had a Met → Leu substitution at codon 134, within the phosphatase domain. The latter mutation was detected by a change in the pattern of in vitro translation initiation and was not found in >50 other alleles tested. However, Met-134 is not required for phosphatase activity (Fig. 3B), so this alteration could be a polymorphism. With one exception (DU145), all of the cell lines retained a mutant *PTEN* allele and lost the other allele, indicating that these cells are null for *PTEN*.

To determine whether *PTEN* mutations are present in primary tumors, we screened genomic DNA from 18 primary glioblastomas for mutations in three exons (21). Mutations in *PTEN* were found in three of these tumors: a 2-bp insertion at codon 15 (534 T), a point mutation resulting in a Gly → Arg change at codon 129 (132T), and a 4-bp frameshift mutation at codon 337 (134T) (Table 1 and Fig. 4D). The mutation at codon 129 is within the signature sequence for tyrosine phosphatases (Fig. 3B). All three tumors appeared to have

LOH in the *PTEN* region since the wild-type allele was substantially reduced in intensity. In addition, the tumor mutations were not detected in paired blood DNA.

In summary, we detected homozygous deletions, frameshift, or nonsense mutations in *PTEN* in 63% (5/8) of glioblastoma cell lines, 100% (4/4) of prostate cancer cell lines, and 10% (2/20) of breast cancer cell lines. These frequencies are likely to be underestimates since the cell lines were not systematically screened for point mutations. We screened xenografts only for homozygous deletions in *PTEN* and detected them in 24% (8/34) of glioblastoma xenografts and 5% (2/40) of breast cancer xenografts. Finally, we detected *PTEN* mutations in 17% (3/18) of primary glioblastomas; this frequency is also likely to be an underestimate since the entire coding sequence was not analyzed. The results of these preliminary screens suggest that a large fraction of glioblastomas and advanced prostate cancers may harbor *PTEN* mutations, whereas the mutation frequency in breast cancer may be lower. Future systematic analysis of all tumor types will be of interest.

The likely function of the P-TEN tumor suppressor as an enzyme that removes phosphate from tyrosines is intriguing, given that many oncoproteins function in the reverse process—to phosphorylate tyrosines (22). P-TEN and tyrosine kinase oncoproteins may share substrates and the tight control of these substrates through phosphorylation is likely to regulate a critical pathway that is altered late in tumor development. The homology of P-TEN to tensin is also of interest. Tensin appears to bind actin filaments at focal adhesions—complex-

es that contain integrins, focal adhesion kinase (FAK), Src, and growth factor receptors (23). Integrins have been implicated in cell growth regulation (24) and in tumor cell invasion, angiogenesis, and metastasis (25), so it is conceivable that *PTEN* regulates one or more of these processes. Finally, the identification of P-TEN as a likely tumor suppressor raises the possibility that this protein and its substrates will be useful targets for the development of new therapeutics for cancer.

## REFERENCES AND NOTES

1. S. H. Bigner *et al.*, *Cancer Res.* **48**, 405 (1988); C. D. James *et al.*, *ibid.*, p. 5546; B. K. A. Rasheed *et al.*, *Oncogene* **10**, 2243 (1995).
2. I. C. Gray *et al.*, *Cancer Res.* **55**, 4800 (1995); M. Iltmann, *ibid.* **56**, 2143 (1996); T. Trybus, A. Burgess, K. Wojno, T. Glover, J. Macoska, *ibid.*, p. 2263.
3. S. Hsu *et al.*, *ibid.* **56**, 5684 (1996).
4. N. A. Lisitsyn and M. Wigler, *Science* **259**, 946 (1993); M. Schutte *et al.*, *Proc. Natl. Acad. Sci. U.S.A.* **92**, 5950 (1995). FDA was performed as described in N. A. Lisitsyn *et al.* (*ibid.*, p. 151). Diploid and aneuploid nuclei from primary breast cancer cells were separated with a fluorescence-activated cell sorter. DNA (100 ng) from each fraction was digested with Bgl II and used to prepare amplicons for 12 separate RDA reactions. Probe CY17 was isolated from one of these reactions. CY17 was 236 bp long and was present in the diploid but not in the aneuploid amplicon from which it was derived. Hybridization of CY17 to normal genomic DNA samples digested with Bgl II revealed no evidence of restriction length polymorphism.
5. D. R. Cox, M. Burmeister, E. R. Price, S. Kim, R. M. Myers, *Science* **250**, 245 (1990). We generated primers to amplify CY17 and screened the GeneBridge4 radiation hybrid panel. The primers were 5'-ATCTAGTGTGAGTTGGGGACAGAGG-3' and 5'-CTGGGTAGGGATTCTGCTCAG-3'. Amplification conditions were 95°C for 30 s, 56°C for 1 min, and 70°C for 1 min for 35 cycles.
6. T. J. Hudson *et al.*, *Science* **270**, 1945 (1995).
7. The CEPH (Centre d'Etude du Polymorphisme Humain) B library (Research Genetics, Huntsville, AL) was screened by PCR using a series of tiered pools to identify unique clones.
8. The forward PCR primer was labeled with [<sup>32</sup>P]ATP and used to amplify 40 ng of genomic DNA. The samples were then subjected to electrophoresis and autoradiography. The samples included 25 human breast tumor cell lines available from American Type Culture Collection (ATCC) as well as 40 human primary breast tumors xenografted into nude mice. The cell lines were HS578T, SK-BR-3, UACC812, UACC893, MDA-MB-453, MDA-MB-175-VII, MDA-MB-468, MDA-MB-361, MDA-MB-231, MDA-MB-436, MDA-MB-415, MDA-MB-330, MDA-MB-157, MDA-MB-134-VI, MDA-MB-435S, ZR 75-30, ZR 75-1, BT-549, BT-483, T-47D, BT-474, DU4475, CAMA1, MCF7, and BT-20.
9. U. Kim *et al.*, *Genomics* **34**, 213 (1996). Clones were isolated from a BAC library (Research Genetics) using AFMA086WG9 as an STS probe.
10. BAC DNA was prepared using the Nucleobond kit (Nest Group, Southboro, MA). BACs were digested with Not I and subjected to electrophoresis on a field inversion apparatus. BACs A, B, C, and D were 240, 200, 175, and 120 kb, respectively (see Fig. 1B). A Not I site was present 20 kb from one end of BAC D. Twelve new STS sites were generated by sequencing both ends of BACs B, C, and D, and shotgun cloning Eco RI fragments. Plasmid DNA was prepared from the cloned Eco RI fragments. DNA was cycle sequenced with appropriate primers using a [<sup>33</sup>P]ddNTP cycle sequencing kit (Amersham). STS primers were designed and the relative location of the STSs determined by testing for their presence in

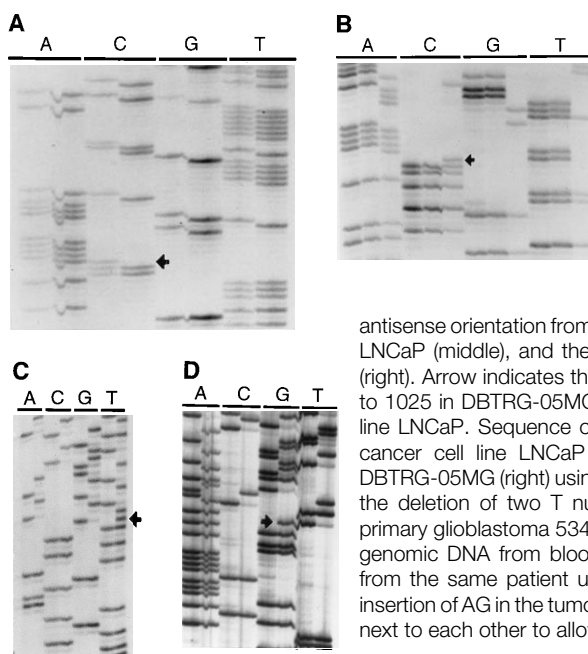


**Fig. 4.** Mutations of *PTEN* in cancer cell lines and primary tumors. **(A)** Mutation in breast cancer cell line BT549. Sequence of nucleotides 831 to 785 (bottom to top) using an antisense primer shows a deletion of a C (arrow) in sample on the right (BT549) but not in the sample on the left (breast cancer cell line ZR-75-30). **(B)** Mutation in glioblastoma cell line DBTRG-05MG. Sequence of nucleotides 1039 to 1010 in the antisense orientation from prostate cancer cell lines DU145 (left), LNCaP (middle), and the glioblastoma cell line DBTRG-05MG (right). Arrow indicates the in-frame deletion of nucleotides 822 to 1025 in DBTRG-05MG. **(C)** Mutation in prostate cancer cell line LNCaP. Sequence of nucleotides 34 to 2 of the prostate cancer cell line LNCaP (left) and the glioblastoma cell line DBTRG-05MG (right) using an antisense primer. Arrow indicates the deletion of two T nucleotides in LNCaP. **(D)** Mutation in primary glioblastoma 534. Sequence of nucleotides 26 to 63 of genomic DNA from blood (left) and primary tumor 534 (right) from the same patient using a sense primer. Arrow indicates insertion of AG in the tumor DNA. A, C, G, and T lanes are loaded next to each other to allow better detection of mutations.

- the BAC contig. Primer sequences are available upon request.
11. The glioblastoma lines included U105, U118MG, A172, DBTRG-05MG, U373MG, T-98G, U-87MG, and U138MG and 34 glioblastoma xenografts. The prostate cancer cell lines tested were DU145, LN-CaP, NCI H660, and PC-3, and microsatellite analysis revealed that each was unique. With the exception of U105, all lines were obtained from ATCC.
  12. DNA (10  $\mu$ g) was digested with Eco RI, resolved on a 1% agarose gel, and transferred to nylon. The JL25 3-kb probe and the 2-kb control probe were randomly labeled and hybridized to the blot consecutively.
  13. A. J. Buckler *et al.*, *Proc. Natl. Acad. Sci. U.S.A.* **88**, 4005 (1991); G. Lennon, C. Auffray, M. Polymeropoulos, M. B. Soares, *Genomics* **33**, 151 (1996). BACs C and D were digested with Bam HI, Bgl II, or both enzymes and then ligated into the trapping vector pSPL3. Libraries were transfected into COS1 cells with lipofectamine and polyadenylated RNA was extracted after 2 days. An exon trapping kit was purchased from GIBCO/BRL.
  14. The map panel #2 monochromosome panel was purchased from the National Institute of General Medical Science (NIGMS) Human Mutant Genetic Cell Repository.
  15. N. K. Tonks and B. G. Neel, *Cell* **87**, 365 (1996).
  16. E. B. Fauman and M. A. Saper, *Trends Biochem. Sci.* **21**, 413 (1996); Z. Sheng and H. Charboneau, *J. Biol. Chem.* **268**, 4728 (1993).
  17. R. H. Diamond, D. E. Cressman, T. M. Laz, C. S. Abrams, R. Taub, *Mol. Cell. Biol.* **14**, 3752 (1994); E. Hogan and D. Koshland, *Proc. Natl. Acad. Sci. U.S.A.* **89**, 3098 (1992).
  18. D. T. Haynie and C. P. Ponting, *Protein Sci.* **5**, 2643 (1996).
  19. J. M. Denu, J. A. Stuckey, M. A. Saper, J. E. Dixon, *Cell* **87**, 361 (1996).
  20. S. M. Powell *et al.*, *N. Engl. J. Med.* **329**, 1982 (1993); P. A. M. Roest, R. G. Roberts, S. Sugino, J. B. van Ommen, J. T. den Dunnen, *Hum. Mol. Genet.* **2**, 1719 (1993). Randomly primed cDNA was prepared from each of the cell lines studied. Reverse transcription (RT)-PCR reactions were performed with two overlapping primer pairs to screen the entire ORF. Primer pairs were as follows: 5'-GGATCCTAATACGACTCACTATAGGGAGACCACCATGGAGTCGCCTGTACACCATTT-C-3' and 5'-TTCCAGCTTTACAGTGAAT TG-3'; 5'-GGATCCTAATACGACTCACTATAGGGAGACCACCATGGGATTTCCCTGCAGAAAG-3' and 5'-TTTTTTCATGGTGTTTATCCCTC-3'. In vitro transcription and translation were performed with the T7 TNT kit (Promega, Madison, WI) and the translation products resolved by electrophoresis. The RT-PCR products that generated truncated proteins were directly cycle sequenced (20 ng each) to identify potential mutations. All mutations were verified by repeating the RT-PCR and mutation analysis. Complementary DNA primer sequences are available upon request.
  21. STSs Not-5', PTPD, and ET-1 were amplified from primary glioblastoma DNA and blood DNA and the exonic regions were sequenced.
  22. T. Hunter, *Cell* **50**, 823 (1987).
  23. J. A. Wilkins, M. A. Risinger, S. Lin, *J. Cell Biol.* **103**, 1483 (1986); J. Z. Chuang, D. C. Lin, S. Lin, *ibid.* **128**, 1095 (1995); S. Miyamoto *et al.*, *ibid.* **131**, 791 (1995); S. Miyamoto, S. K. Akiyama, K. M. Yamada, *Science* **267**, 883 (1995).
  24. X. Zhu, M. Ohtsubo, R. M. Bohmer, J. M. Roberts, R. K. Assoian, *J. Cell Biol.* **133**, 391 (1996); K. K. Wary, F. Mainiero, S. J. Isakoff, E. E. Marcantonio, F. E. Giancotti, *Cell* **87**, 733 (1996).
  25. S. K. Akiyama, K. Olden, K. M. Yamada, *Cancer Metastasis Rev.* **14**, 173 (1995).
  26. We thank B. Vogelstein, N. Tonks, and E. Marcantonio for their comments and S. Kalachikov and R. Hauptschein for helpful suggestions. R.P. is a James S. McDonnell Scholar. M.H.W. is an American Cancer Society Research Professor and is supported by the Department of the Army (DAMD 17-94-I4247), NCI (5R35 CA39829), Amplicon Corporation, and the "1 in 9" breast cancer organization. This work is dedicated to the memory of Richard K. Parsons and Richard P. Sanchez.

3 February 1997; accepted 27 February 1997

# AAAS–Newcomb Cleveland Prize

## To Be Awarded for a Report, Research Article, or an Article Published in *Science*

The AAAS–Newcomb Cleveland Prize is awarded to the author of an outstanding paper published in *Science*. The value of the prize is \$5000; the winner also receives a bronze medal. The current competition period began with the 7 June 1996 issue and ends with the issue of 30 May 1997.

Reports, Research Articles, and Articles that include original research data, theories, or syntheses and that are fundamental contributions to basic knowledge or are technical achievements of far-reaching consequence are eligible for consideration for the prize. The paper must be a first-time publication of the author's own work. Reference to pertinent earlier work by the author may be included to give perspective.

Throughout the competition period, readers are

invited to nominate papers appearing in the Reports, Research Articles, or Articles sections. Nominations must be typed, and the following information provided: the title of the paper, issue in which it was published, author's name, and a brief statement of justification for nomination. Nominations should be submitted to the AAAS–Newcomb Cleveland Prize, AAAS, Room 1044, 1200 New York Avenue, NW, Washington, DC 20005, and **must be received on or before 30 June 1997**. Final selection will rest with a panel of distinguished scientists appointed by the editor-in-chief of *Science*.

The award will be presented at the 1998 AAAS annual meeting. In cases of multiple authorship, the prize will be divided equally between or among the authors.